

Interfaces in Superconducting Hybrid Heterostructures with an Antiferromagnetic Interlayer

K. Y. Constantinian^{a,*}, Yu. V. Kisilinskii^a, G. A. Ovsyannikov^{a,b}, A. V. Shadrin^{a,b},
A. E. Sheyerman^a, A. L. Vasil'ev^c, M. Yu. Presnyakov^c, and P. V. Komissinskiy^{a,d}

^a *Kotelnikov Institute of Radio Engineering and Electronics, Russian Academy of Sciences,
ul. Mokhovaya 11–7, Moscow, 125009 Russia*

* e-mail: karen@hitech.cplire.ru

^b *Chalmers University of Technology, Göteborg, 416 96 Sweden*

^c *National Research Centre “Kurchatov Institute,” pl. Akademika Kurchatova 1, Moscow, 123182 Russia*

^d *Technische Universität Darmstadt, Karolinenplatz 5, Darmstadt, 64289 Germany*

Received August 29, 2012

Abstract—The structural, X-ray diffraction, and electrophysical studies of hybrid superconducting heterostructures with an interlayer of cuprate antiferromagnetic $\text{Ca}_{1-x}\text{Sr}_x\text{CuO}_2$ (CSCO) with the upper electrode Nb/Au and the lower electrode $\text{YBa}_2\text{Cu}_3\text{O}_{7-\delta}$ (YBCO) have been carried out. It has been experimentally shown that the epitaxial growth of two cuprates, YBCO and CSCO, results in the formation of an interface on which the enrichment of the CSCO interlayer with charge carriers proceeds to a depth of about 20 nm. In this case, the conduction of the enriched CSCO region proves to be closer to metallic, whereas the CSCO film deposited onto the NdGaO_3 substrate is a Mott insulator with hopping conduction.

DOI: 10.1134/S1063783413030153

1. INTRODUCTION

Since recently, great interest has been expressed in processes of electron transport on the interface between a superconductor (S) and a magnet (M), where a number of nontrivial physical phenomena take place due to the interaction between superconducting and magnetic correlations [1–4]. It should be noted that a significant part of experimental studies of S/M interfaces was conducted on metallic or polycrystalline films [3–5], in which the influence of the crystalline structure of the contacting materials is neutralized. The coherence length of oxide materials, which is substantially smaller than that of metals, significantly complicates the production of oxide superconducting structures with magnetic interlayers. Nevertheless, the anomalous proximity effect in cuprate superconductors was observed in lanthanum structures [6] and a supercurrent of the Josephson nature was experimentally measured in hybrid mesa-heterostructures with an antiferromagnetic interlayer [7, 8]. The decisive significance for observation of the above-mentioned phenomena belongs to crystalline and electrophysical characteristics of the interfaces of contacting materials. In this work, we present the results of structural analysis on a transmission electron microscope and an X-ray diffractometer and the electrophysical characteristics of hybrid $S-M-S'$ mesa-heterostructures (MHS) in which the role of S was played by a superconductor with the s -symmetry of the order parameter, i.e., a thin-film two-layered Nb/Au struc-

ture, the role of the S' -electrode was played by cuprate superconductor $\text{YBa}_2\text{Cu}_3\text{O}_{7-\delta}$ (YBCO) with the dominating d -symmetry of the order parameter, and the role of the M -interlayer was played by antiferromagnet $\text{Ca}_{1-x}\text{Sr}_x\text{CuO}_2$ (CSCO) ($x = 0.15$ or 0.50).

2. MESA-HETEROSTRUCTURES AND STRUCTURAL MEASUREMENTS

The YBCO superconducting film was epitaxially deposited by laser ablation technique at a temperature of 700–800°C onto a $\text{NdGaO}_3(110)$ (NGO) substrate. The critical temperature for YBCO was $T_C = 88$ –89 K. The magnetic M -interlayer was fabricated from cuprate $\text{Ca}_{1-x}\text{Sr}_x\text{CuO}_2$ ($x = 0.15$ or 0.50), which is a Heisenberg antiferromagnet. A thin (5–50 nm) film of the M -interlayer was epitaxially grown over YBCO in the same vacuum chamber at a high temperature and, then, covered with a thin (20–30 nm) layer of gold after cooling to room temperature [7]. Cuprate YBCO and CSCO films have close crystal parameters and good chemical compatibility. The basal plane parameter in YBCO, $a = 0.3859$ nm, is close the a -parameter in CSCO: $a = b = 0.385$ nm. The parameter $c = 0.318$ – 0.323 nm in the M -interlayer varies depending on the Sr content ($x = 0.15$ or 0.50) [9]. The data on interplanar (along the c axis) distances a_\perp are summarized in the table. The deposition of the two-layered superconducting Nb/Au structure over the M -interlayer makes it possible to obtain Josephson junctions,

Crystallographic parameters and rocking curve widths (a_{\perp} is the interplanar distance in the direction of the c axis, and $\Delta\omega$ is the rocking curve width measured at the half-maximum)

Parameter	CSCP ($x = 0.15$)	CSCO/YBCO ($x = 0.15$)		CSCO ($x = 0.5$)	CSCO/YBCO ($x = 0.5$)	
	CSCO(002)	CSCP(002)	YBCO(007)	CSCP(002)	CSCO(002)	YBCO(007)
a_{\perp} , nm	0.321	0.322	1.169	0.333	0.336	1.177
$\Delta\omega$	0.07	0.2*	0.2*	0.4	0.5*	0.5*

* The estimate of $\Delta\Omega$ from $2\theta/\omega$ -scan without regard for the film thickness.

whose microwave and magnetic properties were studied earlier [10, 11]. The topology of Josephson junctions in the form of a square with the linear sizes $L = 10\text{--}50\ \mu\text{m}$ was formed by ion-beam and reactive etching techniques.

The samples for studying the cross section of the heterostructure were fabricated on a Helios (FEI, United States) electron-ion microscope by means of a focused ion beam with the energy of 30 kV in the beginning and 2 kV in the end of the process. The electron microscopy studies were performed on a TITAN 80-300 transmission scanning electron microscope supplied with an EDAX (United States) energy-dispersive X-ray microanalyzer, a GIF (Gatan, United States) energy filter, and a high-angle dark-field electron detector (Fischione, United States) under an accelerating voltage of 300 kV. A light-field image of the cross section of the heterostructure, obtained by means of the transmission electron microscope, is shown in Fig. 1. We can clearly see the YBCO/NGO and Au/CSCO interfaces. The inset in the same figure

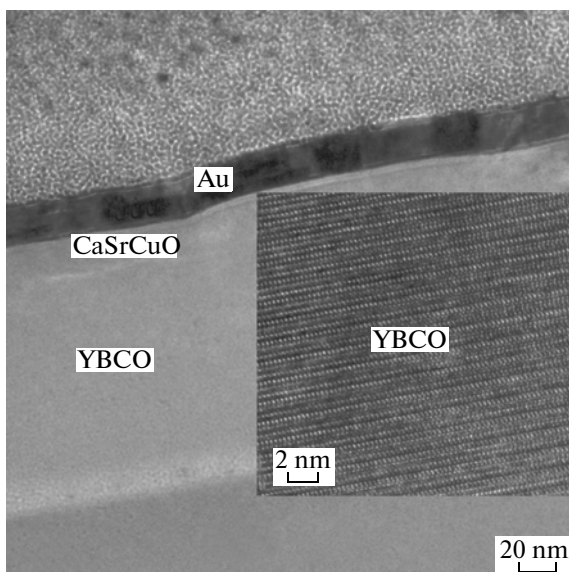


Fig. 1. Light-field transmission electron microscope image of the cross section of an Au/CSCO/YBCO/NGO heterostructure. The inset shows the section of the YBCO film on an enlarged scale.

shows a section of the YBCO film. The results of the microanalysis of composition by the EDAX (Fig. 2), indicate the presence of Ca and Sr in the interval 175–195 nm, i.e., in the range of thicknesses of the M -interlayer, estimated from the number of laser ablation pulses by means of the calibration of the CSCO film growth rate.

3. ELECTROPHYSICAL CHARACTERISTICS

Figure 3 shows the dependences of the resistivity ρ on the temperature of CSCO films with $x = 0.15$ and 0.50, deposited onto an NGO substrate. The dependences $\rho(T)$ correspond to a three-dimensional hopping conductivity with the exponent of the inverse temperature of $1/4$,

$$\ln\rho(T) = \ln\rho_0 + (T_0/T)^{1/4}, \quad (1)$$

where $T_0 = 24/(\pi k_B N_F a^3)$ is an experimental parameter [12], N_F is density of states at the Fermi level, a is the radius of localization of carriers, and k_B is the Boltzmann constant. For CSCO film with $x = 0.5$, we obtain $T_0 = 3 \times 10^6$ K and the resistivity ρ at low tem-

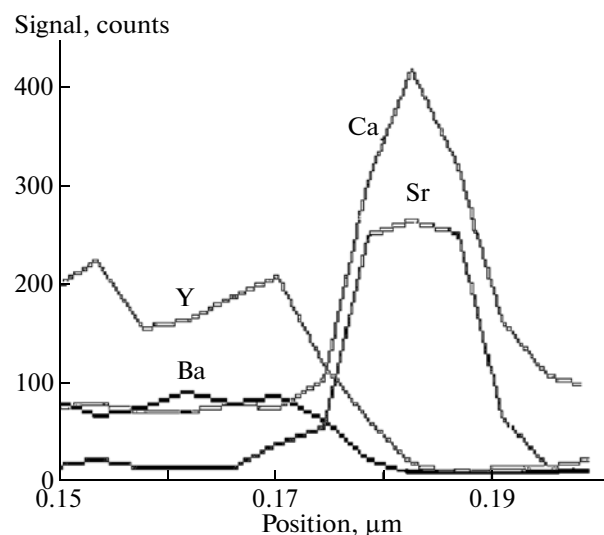


Fig. 2. Results of the energy-dispersive X-ray microanalysis of the cross section of an MHS near the CSCO/YBCO interface.

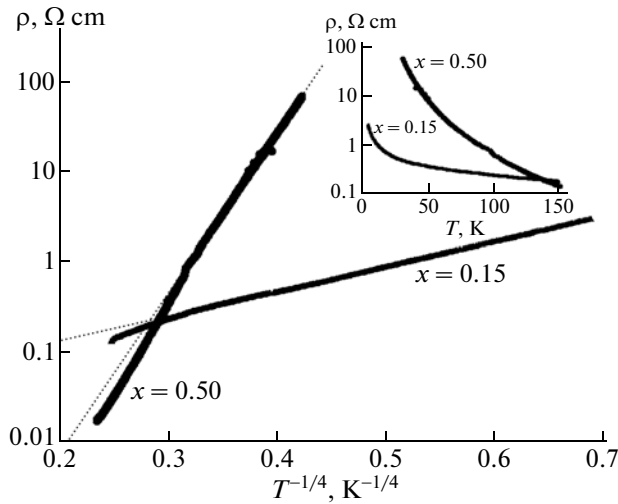


Fig. 3. Temperature dependences of the resistivity of CSCO ($x = 0.50$ and 0.15) films. Dotted lines represent the result of extrapolation of $\rho \sim T^{1/4}$. The inset shows the same dependences plotted on the linear scale with respect to temperature.

peratures of $10^4 \Omega \text{ cm}$. It should be noted that, in all studied CSCO films, no metallic behavior of conductivity has been found.

The resistance (R) of the MHS is the sum of the resistances of the YBCO electrode, the M /YBCO interface, the M -interlayer, the barrier between the M -interlayer and Au, and the YBCO electrode: R_Y , $R_{M/Y}$, R_M , R_b , and $R_{\text{Nb/Au}}$, respectively. Figure 4 shows the temperature dependence $R(T)$ of the resistance of an MHS with $d_M = 20 \text{ nm}$, $x = 0.5$, and $L = 10 \mu\text{m}$. The resistivity of the Nb/Au metallic electrode at room temperature is $\rho_{\text{Nb/Au}} = 10^{-5} \Omega \text{ cm}$ for a thickness $d_{\text{Nb/Au}} = 120 \text{ nm}$; hence, at temperatures below the critical temperature of the YBCO electrode ($T < T_C$), the contribution of the resistance $R_{\text{Nb/Au}}$ is small. At temperatures below the critical temperature of the Nb/Au electrode, $T_C = 8\text{--}9 \text{ K}$, the resistance $R_{\text{Nb/Au}} = 0$. At temperatures $T > T_C$, the dependence $R(T)$ of the MHS is similar to the separately measured dependence $R_Y(T)$ of YBCO film. We can see that, with a decrease in temperature, after YBCO have passed to the superconducting state (in the given case, at $T_C \cong 62 \text{ K}$), for $T_C < T < T_C$, the dependence $R(T)$ has a section of with a practically unchanged resistance $R = R_{M/Y} + R_M + R_b$. Taking into account the epitaxial growth of two cuprates, CSCO/YBCO, and close parameters of their crystal lattices, we assume that the resistance $R_{M/Y}$ is small compared with R_b . Therefore, in the light-field image (Fig. 1), we can clearly see a color contrast of CSCO/Au interfaces, whereas the YBCO/CSCO is hardly distinguishable. The inset in Fig. 4 shows the dependence of $R_N A$ on the thickness d_M for MHS in which the Josephson effect is observed

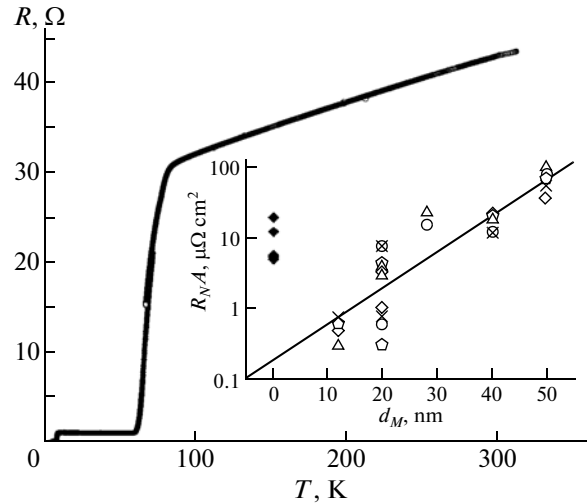


Fig. 4. Temperature dependence of the resistance of CSCO with an interlayer thickness of 20 nm and $L = 10 \mu\text{m}$. The inset shows the dependence of the characteristic resistance $R_N A$ on the thickness of CSCO ($x = 0.5$) interlayer at $T = 4.2 \text{ K}$. Closed symbols indicate the case when the magnetic interlayer is absent and when the MHS has an interlayer with thicknesses $L = (\times) 10, (\circ) 20, (\Delta) 30, (\diamond) 40$, and $(\circ) 50 \mu\text{m}$.

(R_N is the resistance in the normal state, measured under a voltage $V \sim 1.5 \text{ mV}$ ($T = 4.2 \text{ K}$), and $A = L^2$ is the area of the MHS). It is evident from the data presented in Fig. 3 that the resistivity ρ_M of autonomous CSCO film ($x = 0.5$) increases with a decrease in temperature. At a temperature $T = 4.2 \text{ K}$, the expected contribution to $R_N A = \rho_M d_M$ from the CSCO film must be more than $10^4 \mu\Omega \text{ cm}^2$. However, in MHS with a relatively thin interlayer ($d_M < 20 \text{ nm}$), no such large values of $R_N A$ were observed. Moreover, as compared to autonomous CSCO film, the resistance of the MHS in the interval $T_C < T < T_C$ weakly depends on temperature. Hence, the main contribution to the resistance of the MHS at low temperatures and small interlayer thicknesses is from the CSCO/Au interface. As is evident from the inset in Fig. 4, the characteristic resistance $R_N A$ of the samples exponentially increases with an increase in d_M : $R_N A = A_R \exp(d_M/a_R)$. The adjustable parameters were calculated by the least-squares method and comprised $a_R = 8.5 \text{ nm}$ and $A_R = 0.184 \mu\Omega \text{ cm}^2$. The obtained data show that, at an interlayer thickness $d_M < 40 \text{ nm}$, the $R_N A$ is smaller than in structures without an M -interlayer ($d_M = 0$). If the main contribution to the resistance of the MHS was from the resistance of the CSCO interlayer, the $R_N A$ would linearly increase with d_M , but this is not observed in the experiment.

Additional information on the electric properties of the interlayer and the YBCO/Au interface can be extracted from the dependence of the capacitance (C) of the MHS on the thickness d_M . The current–voltage

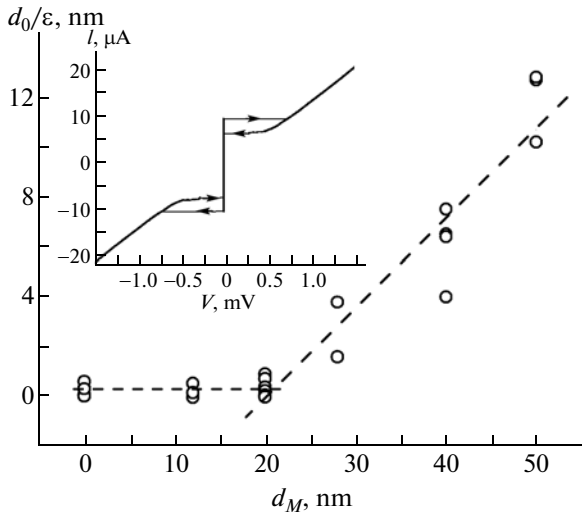


Fig. 5. Dependence of the normalized barrier thickness (d_0/ε) on the $\text{Ca}_{1-x}\text{Sr}_x\text{CuO}_2$ interlayer thickness (d_M) for $x = 0.5$. Lines are the approximated dependences. The inset shows the current–voltage characteristic of the MHS with a thickness of the $\text{Ca}_{1-x}\text{Sr}_x\text{CuO}_2$ interlayer $d_m > 20$ nm. Arrows indicate the critical current and the return current.

characteristics of Josephson MHS at $T = 4.2$ K exhibited hysteresis (see inset in Fig. 5). The capacitance was found from the value of the McCumber parameter $\beta_C = 4\pi e I_C R_N^2 C/h$, which is uniquely related to the ratio of the returned current to the critical current of the current–voltage characteristic of the Josephson junction [13]. For the planar geometry of the MHS, the capacitance is $C = \varepsilon_0 \varepsilon A/d_0$, where ε_0 is the permittivity of the vacuum, ε is the permittivity of the CSCO/Au barrier layer, and d_0 is the barrier thickness. Figure 5 shows the dependence of d_0/ε on the thickness d_M of the CSCO interlayer. We can see that, for $d_M \leq 20$ nm, the variation in the capacitance is insignificant and the value of d_0/ε (for series of MHS with $d_M = 12$ and 20 nm) is the same, within the error, as in the case of heterostructures without an interlayer: $d_0/\varepsilon = 0.35 \pm 0.20$ nm.

The presence of hysteresis in heterostructures without an interlayer [14] indicates the formation of a barrier layer on the YBCO/Au interface, which determines the value of the capacitance between the YBCO and NbAu electrodes. In the case of an MHS, the barrier layer is formed on the CSCO/Au interface. Let us analyze what role is played in this case by the CSCO layer. For $d_M > 20$ nm, an increase in d_0/ε is observed in several series of MHS. Using the least-squares method, we obtain for the increasing section the linear dependence $d_0/\varepsilon = (0.36 \pm 0.05)[d_M - (20 \pm 4)]$ nm. Such a dependence of d_0/ε on d_M is described by a model in which, under the influence of YBCO, a conducting layer is formed on the CSCO/YBCO inter-

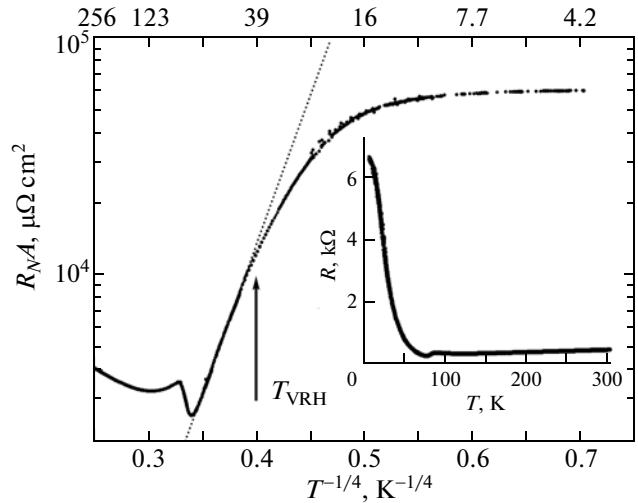


Fig. 6. Temperature dependences of the characteristic resistance of the MHS ($x = 0.5$, $d_M = 80$ nm, $L = 30$ μm). The arrow indicates the temperature T_{VRH} below which the temperature interval corresponds to the mechanism of conduction (1) (dotted line), $T_0 = 7 \times 10^5$ K. The inset shows the temperature dependence (on the linear scale) of the conductivity of the same MHS.

face, which does not contribute to the capacitance C . Over the conducting CSCO layer (with a thickness up to 20 nm), the weakly conducting part of the CSCO interlayer with a thickness d_0 is situated, which determines the capacitance of the MHS. It should be noted that, although the characteristic resistances $R_N A$ of MHS and heterostructures without an M -interlayer differ almost by an order of magnitude (see inset in Fig. 4), the values of d_0/ε are practically equal for $d_M < 20$ nm. Earlier, the emergence of a conductive layer (with a thickness up to 50 nm) was observed for other cuprates on the $\text{PrBa}_2\text{Cu}_3\text{O}_7/\text{YBCO}$ interface [15]. It is known that, in thin CSCO films, reconstruction of the electron subsystem can take place due to oxygen nonstoichiometry [16–18]. As was shown in [16], despite a weak cation diffusion (1–2 atomic cells), the alteration of the conductivity of contacting materials on the interface of two oxides can be caused by electron reconstruction, as it takes place on the interface between a strong Mott insulator and a insulator with a gap in the excitation spectrum [16]. The charge reconstruction due to a reduction in the oxygen content in the film during its growth [18] can lead to a significantly change in the electron subsystem of the CSCO layer and transition to the metallic state. The assumption that the main contribution to the resistance of MHS is made by the CSCO/Au interface is supported by the difference in the conductivities, Fermi velocities, and crystallographic parameters of the contacting materials and by the presence of defects on the interface.

At relatively large $d_M > 70$ nm, a dramatic change in the $R(T)$ of MHS took place (see inset in Fig. 6). In this case, the contribution from the resistance of the barrier, R_b , is no large compared to R_M , and the resistance of the CSCO film makes an exponential (with an increase in d_M) contribution to $R_N A$.

In the interval of temperatures $T = 70\text{--}43$ K, a dependence described by (1) was observed, which is typical for hopping conductivity. The value of the adjustable parameter, $T_0 = 7 \times 10^5$ K turned out to be several times smaller than that for autonomous CSCO film. If the hop length $2r \cong a(T_0/T)^{1/4}$ becomes comparable with the barrier thickness, then the mechanism of conduction in MHS can change, e.g., from hopping to tunneling through localized states [12, 19]. In Fig. 6, this temperature, at which the hop length $2r$ becomes equal to d_0 and the mechanism of conduction change, is denoted by T_{VRH} . From the data presented in Fig. 6, we have $T_{\text{VRH}} = 43$ K and, for $d_M = 80$ nm, taking into account the dependence of d_0/ε on d_M (Fig. 5), we obtain $d_0 = 60$ nm and the radius of localization $a \cong 5$ nm. Using the values of T_0 and a from the relation $T_0 = 24/(\pi k_B N_F a^3)$, we find the state density $N_F = 10^{18}$ eV $^{-1}$ cm $^{-3}$, which is substantially lower than that observed in PrBa $_2$ Cu $_3$ O $_7$ [15].

4. CONCLUSIONS

Thus, as a result of the structural, X-ray diffraction, and electrophysical studies of hybrid mesa-heterostructures based on a cuprate semiconductor (YBCO) with an interlayer of cuprate antiferromagnet (CSCO), it has been established that the epitaxial growth of two cuprates, YBCO and CSCO, an interface with a high transparency. In the autonomous case, when a CSCO film is applied immediately onto the substrate, the material of the interlayer is a Mott insulator with hopping conductivity but, on the YBCO/CSCO interface, the CSCO film is doped with charge carriers to the depth of about 20 nm to a state close to metallic, which leads to a reduction in the resistivity of MHS with a CSCO interlayer as compared to the resistivity of an autonomous CSCO film by two orders of magnitude. At the interlayer thicknesses more than 70 nm, the resistance of MHS in a certain temperature interval has a dependence typical for hopping conductivity, from which we succeeded in estimating the characteristic temperature of the hopping conductivity and the state density on the Fermi level for the interlayer.

ACKNOWLEDGMENTS

We are grateful to I.V. Borisenko, V.V. Demidov, A.V. Zaitsev, A. Kalabukhov, I.M. Kotelyanskii, and A.M. Petrzhik for their assistance in performing the experiment and helpful discussions.

This study was supported by the Department of Physical Sciences of the Russian Academy of Sciences, the Ministry of Education and Science of the Russian Federation (grant no. 02.740.11.0795), the Council on Grants from the President of the Russian Federation (grant no. NSh-2456.2012.2), the Russian Foundation for Basic Research (project nos. 11-02-01234a and 12-07-31207mol_a), and the Visbi program of the Swedish Institute.

REFERENCES

1. A. Buzdin, Rev. Mod. Phys. **77**, 935 (2005).
2. F. S. Bergeret, A. F. Volkov, and K. B. Efetov, Rev. Mod. Phys. **77**, 1321 (2005).
3. V. V. Ryazanov, V. A. Oboznov, A. Y. Rusanov, A. V. Vretennikov, A. A. Golubov, and J. Aarts, Phys. Rev. Lett. **86**, 2427 (2001).
4. M. Flokstra and J. Aarts, Phys. Rev. B: Condens. Matter **80**, 144513 (2009).
5. C. Bell, E. J. Tarte, G. Burnell, C. W. Leung, D.-J. Kang, and M. G. Blamire, Phys. Rev. B: Condens. Matter **68**, 144517 (2003).
6. A. Gozar, G. Logvenov, L. F. Kourkoutis, A. T. Bollinger, L. A. Giannuzzi, D. Muller, and I. Bozovic, Nature (London) **455**, 782 (2008).
7. A. V. Zaitsev, G. A. Ovsyannikov, K. Y. Constantinian, Yu. V. Kislinskii, A. V. Shadrin, I. V. Borisenko, and F. V. Komissinskiy, JETP **110** (2), 336 (2010).
8. G. A. Ovsyannikov and K. Y. Constantinian, Low Temp. Phys. **38** (4), 333 (2012).
9. G. A. Ovsyannikov, C. A. Denisyuk, and I. K. Bdikin, Phys. Solid State **47** (3), 429 (2005).
10. Y. V. Kislinskii, K. Y. Konstantinyan, G. A. Ovsyannikov, F. V. Komissinskiy, I. V. Borisenko, and A. V. Shadrin, JETP **106** (4), 800 (2008).
11. G. A. Ovsyannikov, K. Y. Constantinian, Yu. V. Kislinskii, A. V. Shadrin, A. V. Zaitsev, A. M. Petrzhik, V. V. Demidov, I. V. Borisenko, A. V. Kalabukhov, and D. Winkler, Supercond. Sci. Technol. **24**, 055012 (2011).
12. Y. Xu, D. Ephron, and M. R. Beasley, Phys. Rev. B: Condens. Matter **52**, 2843 (1995).
13. H. H. Zappe, J. Appl. Phys. **44**, 1371 (1973).
14. P. V. Komissinskiy, G. A. Ovsyannikov, K. Y. Constantinian, Y. V. Kislinski, I. V. Borisenko, I. I. Soloviev, V. K. Kornev, E. Goldobin, and D. Winkler, Phys. Rev. B: Condens. Matter **78**, 024501 (2008).
15. M. I. Faley, U. Poppe, C. L. Jia, and K. Urban, IEEE Trans. Appl. Supercond. **7**, 2514 (1997).
16. S. Okamoto and A. Millis, Nature (London) **428**, 630 (2004).
17. J. C. Nie, P. Badica, M. Hirai, J. Y. Kodama, A. Crisan, A. Sundaresan, Y. Tanaka, and H. Ihara, Physica C (Amsterdam) **388–389**, 441 (2003).
18. S. J. L. Billinge, P. K. Davies, T. Egami, and C. R. A. Catlow, Phys. Rev. B: Condens. Matter **43**, 10340 (1991).
19. U. Kabasawa, Y. Tarutani, M. Okamoto, T. Fukazawa, A. Tsukamoto, M. Hiratani, and K. Takagi, Phys. Rev. Lett. **70**, 1700 (1993).

Translated by E. Chernokozhin